JOURNAL OF MATERIALS SCIENCE 36 (2001) 4883–4891

Thermo-mechanical properties of hyperbranched polymer modified epoxies

R. MEZZENGA, J. A. E. MÅNSON*
Laboratoire de Technologie des Composites et Polymères (LTC), École Polytechnique Fédérale de Lausanne (EPFL), CH-1015 Lausanne, Switzerland
E-mail: jan-anders.manson@epfl.ch

The thermo-mechanical properties of hyperbranched polymer-epoxy blends and their dependence on hyperbranched polymer shell chemistry were investigated. Hyperbranched polymers were shown to be able to increase resin toughness by inducing both a heterogeneous and homogeneous morphology. While the former was better performing in terms of toughness, the latter showed satisfactory toughness together with complete transparency. In order to understand fracture toughness enhancement, toughening mechanisms as well as the properties of both matrix and particles were studied. Particle composition was derived by combining dynamic mechanical analysis and the Fox equation. This resulted in an evaluation not only of particle composition but also of glass transition temperature and stiffness, whose value was cross-checked by a micro-mechanical model. The complete picture concerning particle and matrix properties, as well as toughening mechanisms and their dependence on hyperbranched polymer shell chemistry, finally enabled defining the optimum molecular design of the hyperbranched polymers in order to achieve the desired fracture toughness.

1. Introduction

Most of the favourable properties of thermosets are related to the existence of cross-links between polymer chains, and depend strongly on the cross-link density. The latter, however, is also responsible for the brittleness of thermosets. This brittle behaviour can often limit applications for both the polymers themselves and thermoset-based composites. Over the past 25 years a lot of effort has been devoted to increase the toughness of thermosets [1–4]. One of the most developed approaches is to blend a second tougher polymer with the fragile thermoset. So far, the most studied systems have been epoxy resins modified by either rubber or thermoplastics able to undergo a phase separation during curing, starting by an initially homogeneous solution [5, 6]. In these systems, fracture toughness can be assessed by changing either processing conditions or the modifier content, which in turn will induce different final morphologies [7].

A promising new method of toughening has been proposed by Boogh *et al.* using epoxy functionalised hyperbranched polymers (HBP) as modifiers for epoxy resins [8]. Hyperbranched polymers have been shown to offer unique and promising characteristics such as high functionality, high molecular weight, and low viscosity-to-molecular weight ratio. At the same time, this class of polymers shows unique toughening properties. Hyperbranched polymers in fact offer all the advantages of other traditional modifiers, and can be dissolved into the thermoset resin to give an initially homogeneous blend with phase separation occurring upon curing. Furthermore, the possibility of tailoring the HBP shell chemistry enables synthesising HBPs having different degrees of compatibility with the resin, thus inducing different final morphologies [9, 10]. Therefore, different mechanical properties have to be expected when different chemistries of HBPs are used. Finally, their low viscosity ($\cong$10 Pa*s), attributed to the conformation of the HBP which has less entanglement than traditional linear macromolecules, allows combining good toughening properties with an excellent processability.

Although the performance of thermoset resins as regards toughness has been shown to improve without affecting other properties when blending with HBPs, many points remain unexplained in the toughening process, such as particle properties or the exact nature of the toughening mechanisms. Thus, in order to understand, control and improve the mechanisms responsible for HBP-thermoset toughening and therefore to judge the real potential of these materials, a fundamental study on the specific blending properties of these materials and the factors affecting toughness was carried out. Processing conditions such as curing temperature or pressure, and blend composition are some of the factors which affect the final properties of these blends and their effects have been described elsewhere [11]. On the other hand, the principal objective of this paper is to characterise and understand the physical properties

*Author to whom all correspondence should be addressed.

of HBP-thermoset polymer blends at the solid state, as a function of the real new feature of this class of modifiers: the HBP molecular design. More specifically, a particular effort has been made in order to understand which are the HBP molecular design specifications that will produce optimum toughness in HBP-epoxy blends.

2. Experimental

2.1. Materials

Diglycidyl ether bisphenol A (DGEBA) (Shell Epon 828) was selected as thermoset resin, while isophorone diamine (IPD) (Fluka) was used as cross-link agent. This resin had an infinite glass transition temperature of 170°C, a Young's modulus of 2.85 GPa, and a K_{1c} of 0.6 MPa*m$^{1/2}$. Five different experimental and commercial grades of 3-generation epoxy functionalized HBPs, supplied by Perstorp AB, were used as modifiers in concentrations of 5, 10 and 20 parts per hundred parts of resin (phr). These differed in their epoxy equivalent weights (EEW), (HBP molecular weight divided by the number of epoxy groups grafted onto its shell), and hence in their solubility in the resin, the lowest EEW corresponding to the most soluble HBP. The hyperbranched polymers used in this work are identified by HBP40, HBP60, BE1^{TM}, HBP95, and BE2^{TM} having an EEW of 1050, 841, 563, 408 and 373 g/equivalent respectively, as obtained directly by titration. The stoichiometric ratio of amine-to-epoxy groups, including those grafted onto the HBP shell, was always maintained in order to achieve 100% conversion in all the blends investigated. In order to compare results with more traditional modifiers, a CTBN based rubber, Hycar 1300 × 8, supplied by BF Goodrich was also included in the study.

2.2. Procedures

Mechanical properties were measured at room temperature on samples cured at 100°C and postcured for one hour at 180°C. Young's moduli of the blends (E) were measured by standard tensile tests on a UTS Testsysteme equipment at a crosshead displacement rate of 2 mm/min. Toughness, expressed by K_{1c}, was measured on compact tension standardised specimens at a crosshead displacement rate of 0.5 mm/min. Glass transition temperatures (T_g), identified by the maximum in Tan(δ), were measured by dynamic mechanical analysis (DMA) using a Rheometric RSAII equipment, at a frequency of 1 Hz on a three point bending geometry. Scanning electron microscopy was used for morphological characterization and analysis of toughening mechanisms. To detect eventual variations of mechanical properties within the particles, an Autoprobe Park Instruments atomic force microscope (AFM) was used in taping mode configuration, at a frequency of 6×10^4 Hz. Poisson ratios of resin and blends were measured by laser speckle interferometer on a Newport HC/ESPI system.

3. Results and discussions

3.1. Blend thermo-mechanical properties

The effects of hyperbranched polymer shell chemistry on glass transition temperature and Young's modulus

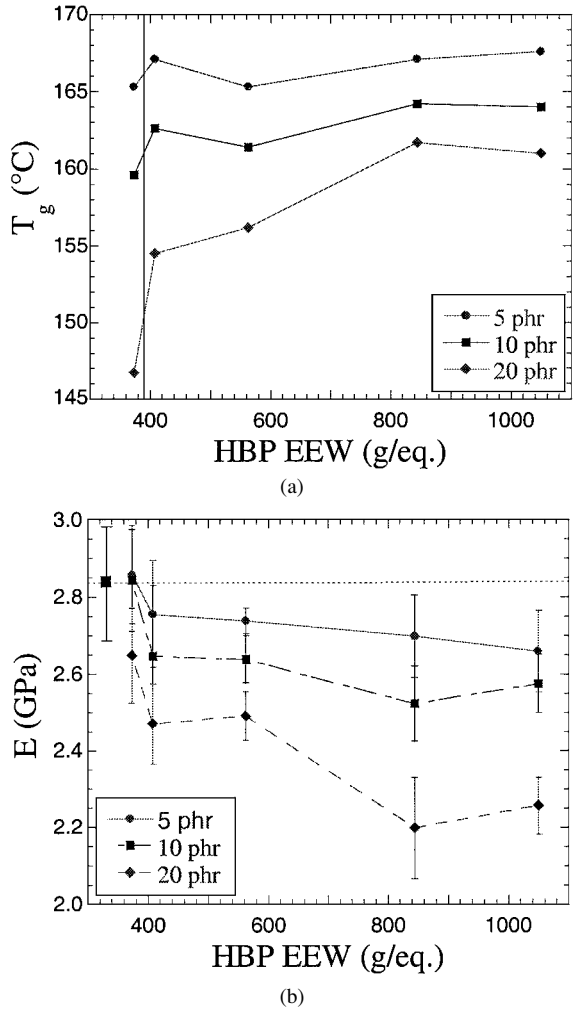

Figure 1 (a) Glass transition temperature and (b) Young's modulus versus hyperbranched epoxy equivalent weight, for three different compositions of HBP in DGEBA-IPD resin.

are shown in Fig. 1, which, for three different concentrations, depicts the dependence of these two properties upon the functionality of the HBP, expressed by the EEW.

With an EEW of 373 g/eq. the blend remained homogeneous at every concentration, and the glass transition temperature was lowered by an amount proportional to the concentration of HBP added (see Fig. 1a). However, as soon as the functionality of the hyperbranched polymer was decreased, phase separation started and the HBP started to be ejected from the continuous phase into separated particles. As a result, the glass transition temperature started to increase and this tendency continued with increasing EEW, with the matrix tending to recover its original value the more and more easily the HBP was ejected. It should be noted here that, unlike the Young's modulus, the glass transition temperature, as measured by DMA, refers to the continuous phase, and its increase with EEW reflects the decrease of residual HBP into the matrix.

Fig. 1b shows the Young's modulus, E, versus the EEW of the HBP blended with the epoxy resin. As can be observed for all the three concentrations, the modulus decreased continuously when the EEW was increased. In this case, the decrease of E with EEW is a consequence of the change in crosslink density of the fully crosslinked different hyperbranched polymers.

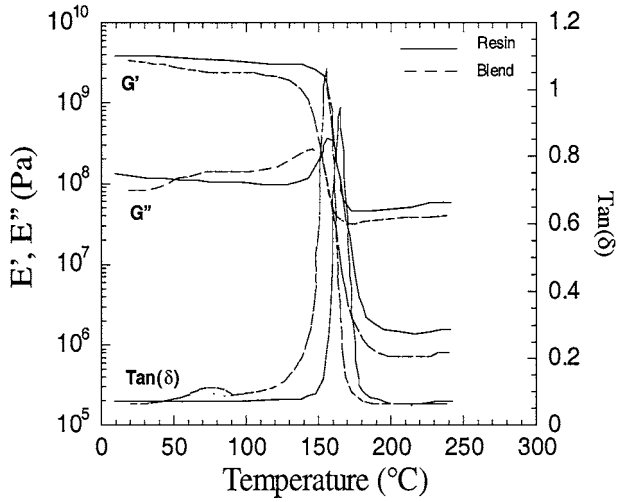

(a)

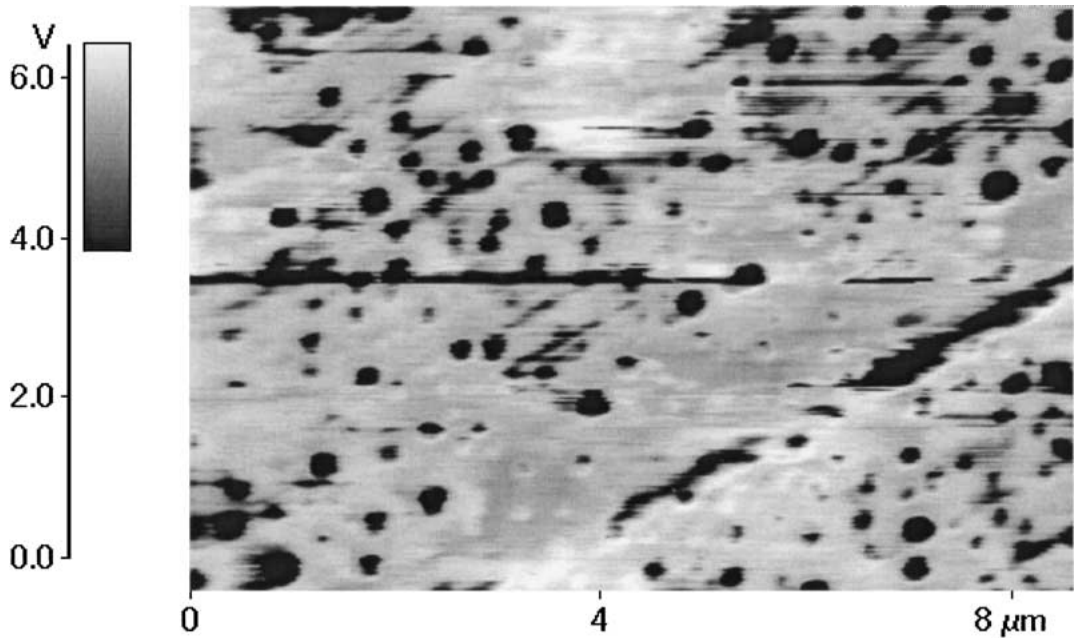

(b)

Figure 2 (a) DMA spectrum for 20 phr of HBP40 in DGEBA-IPD resin. A second transition peak in the region of 60–80°C corresponds to the second domain glass transition temperature. (b) AFM picture of 20 phr of HBP60 in DGEBA-IPD resin. The lack of colour gradient in the signal within the particles indicates particle homogeneity.

In fact, a more functional HBP can achieve a higher crosslink density when fully crosslinked, and thus a higher stiffness.

3.2. Particles properties

Although the glass transition temperature of the continuous phase was easily measured by DMA, this was not the case for second domains obtained with hyperbranched polymers as modifiers. Indeed, only in a few cases a transition peak was identified for the second domains. Fig. 2a is a typical example, showing, for a 20 phr of HBP40 mixed with the epoxy resin, the loss and storage moduli E" and E' together with their ratio Tan(δ). A very spread peak for Tan(δ) is noticeable in the 60–80°C region, which corresponds to the particles glass transition. In all the other cases, a few reasons could be invoked to account for the fact that the second phase peak was hardly identifiable. First of all, it was easier to identify the peak when the morphologies had a mono-disperse particle distribution: in this case in fact, since all the particles started nucleation at similar times they also had similar compositions and therefore similar properties, such as the glass transition temperature. However, in some cases, even very mono-disperse HBP-epoxy blends at high HBP concentrations did not show a very sharp second phase peak. A gradient of properties within the particles, which was suggested by Boogh *et al.* [8] would explain the lack of a sharp second phase transition. On one hand, thermodynamics can justify such a gradient, due to the evolution of particle composition during phase separation. Nevertheless, the full process occurs when the particles are still in the totally liquid state and any composition gradient would be readily averaged by polymer diffusion within the liquid droplets. In this respect, atomic force microscope experiments confirmed the particles to be rather homogeneous, within good approximation as shown in Fig. 2b for a 20 phr of HBP60 blended with the epoxy resin. Thus, the main reason why second phase particles were not easy to identify, especially at high functionality, must be attributed to the high residual solubility of the HBP within the matrix, which broadened the

TABLE I Young's modulus and glass transition temperature of fully crosslinked components

Component	E (MPa)	T_g (°C)
HBP40-IPD	1.5	−16.5
HBP60-IPD	3.7	−0.8
HBP95-IPD	127	27
DGEBA-IPD	2850	170

TABLE II Particle volume fraction and composition, blend Poisson ratio, and particle thermo-mechanical properties for blends of 20 phr HBP in the DGEBA-IPD system

Blend	V_P	ϕ_E	ν	E (GPa)$_{Comp.}$	E (GPa)$_{Mech.}$	T_g (°C)
HBP40	0.29	0.58	0.38	1.60	1.3	65.4
HBP60	0.18	0.4	0.38	1.14	1.1	48.8
HBP95	0.03	≈0	0.36	0.13	≈0	27

main resin peak and led to an overlapping with the second phase domain transition temperature. As a consequence, the procedure used in this work for evaluating particle glass transition temperature had to start by using the data of the continuous phase for which the glass transition temperature was easily measured.

The continuous phase of the blend was considered to be as a homogeneous mixture, whose composition was unknown, of two thermoset components: DGEBA-IPD and HBP-IPD respectively. Thus, if the glass transition temperatures of the two components and of the continuous phase were known (see Table I), the Fox equation [12] allowed the determination of the composition of the blend:

$$\frac{1}{T_g^{\text{eff}}} = \frac{w_E}{T_g^E} + \frac{1 - w_E}{T_g^{HBP}} \quad (1)$$

where T_g^{eff}, T_g^E, T_g^{HBP} are glass transition temperatures of the mixture, the fully cured epoxy and the fully cured hyperbranched polymer respectively, and w_E is the weight fraction of fully cured epoxy in the continuous phase. The applicability of the Fox equation in hyperbranched polymer-epoxy blends was verified by blending the epoxy resin with BE2, whose low EEW (373 g/eq.) led to a homogeneous blend at every concentration. The experimental results shown in Fig. 3, compared with the predictions of Equation 1, indicate a satisfactory agreement between theory and experiments. Now, since the phase-separated volume was known by SEM, a simple mass balance allowed the computation of composition in the second domain phase. Table II reports the composition of second domains for blends of 20 phr of HBP40, HBP60 and HBP95 and epoxy. As can be observed, in the case of low functional HBPs, the second domain particles contained a large amount of epoxy resin, which could be as high as 58%. On the other hand, the epoxy content decreased to almost zero (within the approximation of the method used) for high functional HBPs.

The results concerning the composition, also allowed an evaluation of the thermo-mechanical properties of particles, which are reported in Table II and described below. Concerning the glass transition temperature, the particles were considered to be homogeneously formed by DGEBA-IPD/HBP-IPD in a composition reported in Table II. Thus, their T_g could be calculated by again using the Fox equation within the particles themselves. The results obtained agree with the experiments in the few cases where there was evidence of a second transition peak. In the same way, the stiffness of the particles could be estimated by considering the Young's modulus as a linear function of composition, which was verified for the homogeneous epoxy-BE2 blend, as shown in Fig. 4. Following this approach, particle stiffness was calculated to range from 130 MPa for HBP95 (whose particles had low epoxy content) to 1.6 GPa for HBP40 (where epoxy content was high). As a consequence, depending on the functionality of the HBPs, one could expect not only different particle properties but also the activation of different toughening mechanisms. Since no direct measurement of Young's modulus was possible for second domain particles, the values for particle stiffness estimated by linear extrapolation were cross-checked by solving the Hashin equation for particulate composites at low concentration of dispersed phase [13]:

$$\frac{G_{\text{eff}}}{G_M} = 1 - \frac{15(1 - \nu_M)\left(1 - \frac{G_P}{G_M}\right)}{7 - 5\nu_M + 2(4 - 5\nu_M)\frac{G_P}{G_M}} V_P \quad (2)$$

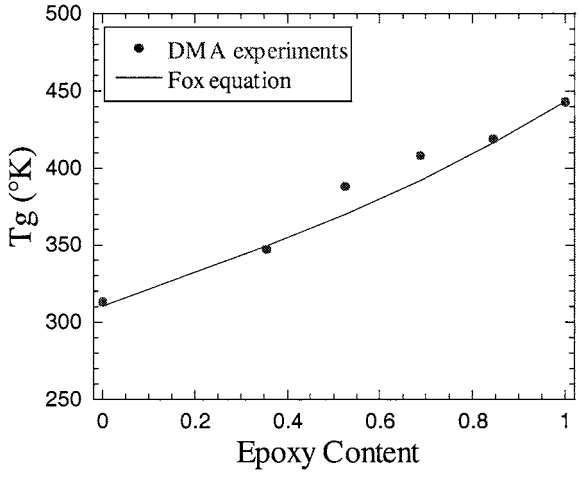

Figure 3 Experimental glass transition temperature and Fox prediction as a function of composition in a homogeneous BE2-DGEBA-IPD blend.

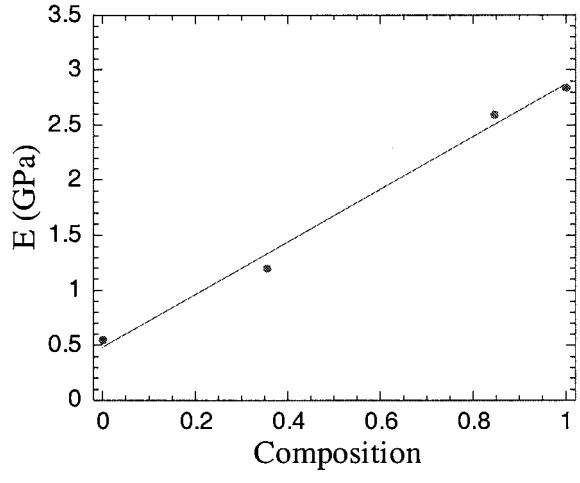

Figure 4 Young's modulus plotted versus composition in a homogeneous BE2-DGEBA-IPD blend.

where G is the shear modulus, V_P is volume fraction of particles in the heterogeneous blend, ν is the Poisson ratio, and the indexes p, eff and M refer respectively to the particles, the blend and the neat resin. For isotropic materials, the values for the shear modulus are related to the Young's modulus by the following expression:

$$E = 2G(1 + \nu) \quad (3)$$

where ν is the Poisson ratio. As it is not possible for particles to be directly measured, the Poisson ratio is normally assumed in the literature to be 0.5, or, when mechanical simulations have to be performed, in the range of 0.5 to 0.5–10^{-3} in order to get the calculations to converge [14–17]. This value, close to 0.5, is supported by the idea of perfectly rubbery-like particles. This was not the case for the blends investigated here, and even in the case of rubber-epoxy blends, the presence of entrapped epoxy within the particles would never led to purely rubbery-like domains. This was confirmed by experimental results, illustrated by Fig. 5, which show the DMA spectrum for the epoxy resin blended with 20 phr Hycar 1300 × 8. It can in fact considerably be noted that the dispersed domain transition occurred at 65°C, indicating particles significantly stiffer than those in purely rubbery domains. Thus, in this work a lower value of 0.45 was assumed for the Poisson ratio of particles. Although, this does not at all influence the final values of Young's modulus reported in Table III, it affects the values of bulk modulus of the particles. As can be seen the values of stiffness predicted with the micromechanical model are in very good agreement with the ones predicted by linear extrapolation of compositions. The higher deviation between two approaches observed for the HBP40, was attributed to the high volume content of particles, whereas Equation 2 applies for low volumes only.

In summary, both the approaches for the Young's modulus calculation, as well as the evaluation of T_g by Fox, highlighted a large range of particle properties, depending on the shell chemistry of the HBP. In the next sections the implications in terms of toughness enhancement and toughening mechanisms are discussed.

TABLE III Properties of DGEBA-IPD blended with 20 phr of HBP60 and Hycar 1300 × 8

	K_{1c} (MPa*m$^{1/2}$)	E (GPA)	T_g (°C)	η^a (Pa*s)
HBP60	1.21	2.49	156.2	13
Hycar 1300 × 8	1.07	2.57	157	135

[a]Viscosity refers to neat modifier.

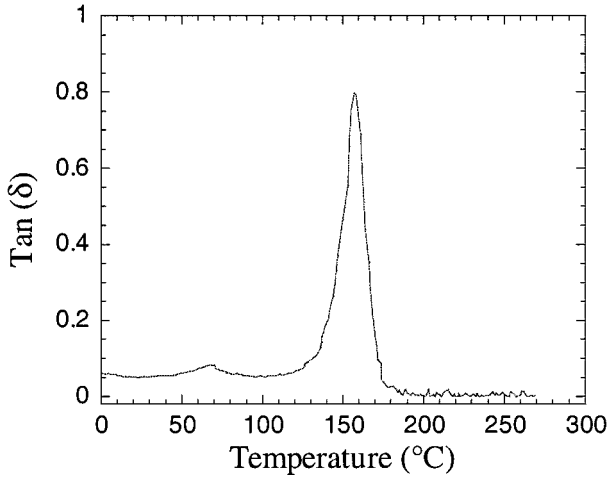

Figure 5 DMA spectrum for 20 phr of Hycar 1300 × 8 in DGEBA-IPD resin.

3.3. Toughening mechanisms

Three main regions were identified in the fractured surface of the compact tension specimens: the pre-crack region, the stable fracture propagation zone, and the unstable fracture zone. The first zone is the region where the pre-crack is introduced by a razor blade. The stable fracture propagation zone is the region within which the toughening mechanisms are active and energy is dissipated before the fracture starts to propagate in a catastrophic manner. Finally the unstable fracture zone is the zone where the fracture propagates in a non-reversible way. In Fig. 6(a) the three regions are distinguished, while in Fig. 6b, the transition between the stable and unstable fracture propagation zone is shown in more detail. The extension of the region, within which the fracture can propagate in a stable manner, provides an indication of the toughness of the resin, since a larger plastic zone will correspond to a larger amount of energy dissipated before the fracture starts to propagate catastrophically [18, 19]. For different HBP-epoxy blend formulations, Fig. 7 illustrates this correspondence between fracture toughness, expressed by K_{1c} and the width of the stable fracture region.

In Fig. 6b it is also clearly shown that when going from the stable fracture propagation zone to the unstable one, the amount of black holes decreased, as well as their size and the roughness of the surface. The black holes are particles which have totally cavitated, i.e. a void has grown within the particles. The change of black hole size and surface roughness when going from one region to the other indicates that the stable fracture propagation zone is the region of most extensive plastic deformation and particle cavitation. By that, it was clearly shown that, as in most modified thermosets, plastic deformation of the matrix and particle cavitation were the main mechanisms leading to improved fracture toughness in HBP-modified epoxies [20–22].

It should be noted that, while in the stable fracture propagation zone almost all particles underwent cavitation, in the unstable region, just a small amount of particles was affected and that in every case, cavitation always appeared to occur in a complete manner. This suggested that within the slow damage zone, enough time was left to activate this toughening mechanism in most of the particles, but, as soon as the fracture started to propagate rapidly, either cavitation did not start at all, or when it did, it occurred very quickly. This is a consequence of the fact that cavitation is a thermally activated mechanism [23], and that, due to the high surface energies of the fully cured particles, which contain considerable amounts of fully crosslinked epoxies and HBPs, high energies of activation must be expected for these particles [24]. Thus, partial cavitation could be

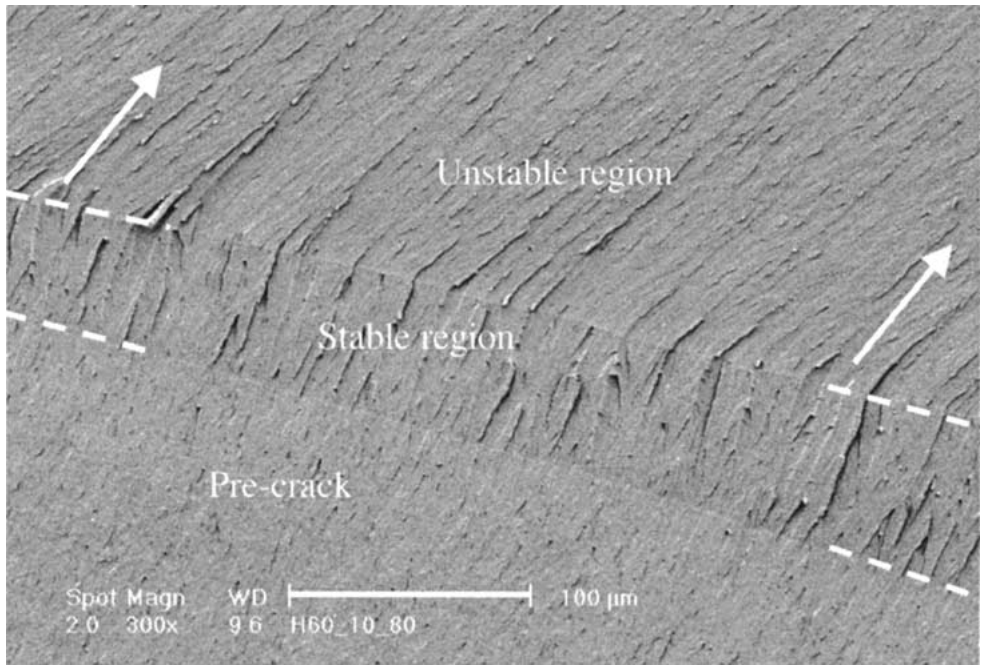

(a)

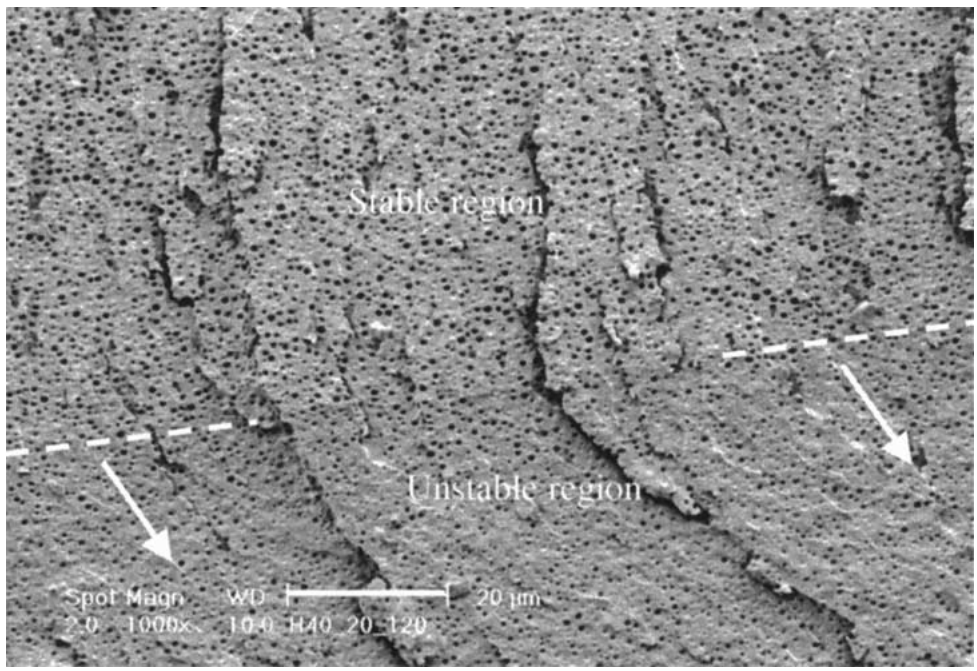

(b)

Figure 6 (a) SEM micrograph showing the precrack region and the stable and the unstable crack propagation region for a blend of 10 phr of HBP60 and DGEBA-IPD. (b) Transition from stable to unstable crack propagation region in a blend of 20 phr of HBP40 and DGEBA-IPD.

observed in few cases and only at the end of the crack pattern, where instantaneous pictures of the toughening mechanisms were provided (see Fig. 8). Finally, in rare cases, particle debonding was observed in the blends investigated. This lack of extensive debonding was attributed to the good interface between the particles and the continuous phase, induced by the HBP high reactivity. A further comment is worth on the shape of particles which have been crossed by the fracture without cavitating. These particles all showed an inflection inwards the surface. This phenomenon, which also has been observed for rubber modified epoxies, is the consequence of the residual tensile stress in which the particles remain after cooling down from curing temperature to room temperature, and is a consequence of their higher coefficient of thermal expansion. This contributes to decrease the energy barrier for particle cavitation [25].

3.4. Toughness increase

Since a high degree of freedom in molecular design is offered with HBP, the main interest of this work is the optimum tailoring of HBP molecular structure to get maximum toughening performances in HBP-epoxy blends. Following this line of thought, the five differently epoxidised three generation hyperbranched polymers described in the experimental part, have allowed a deep understanding.

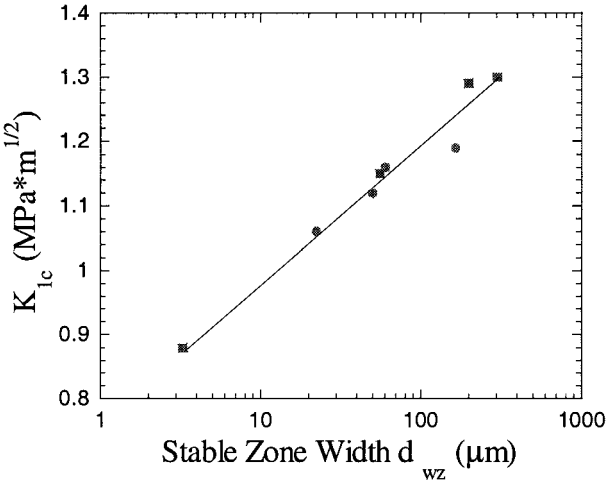

Figure 7 Fracture toughness (K_{1c}), plotted versus the width of the stable fracture propagation zone, for several different experimental blend formulations.

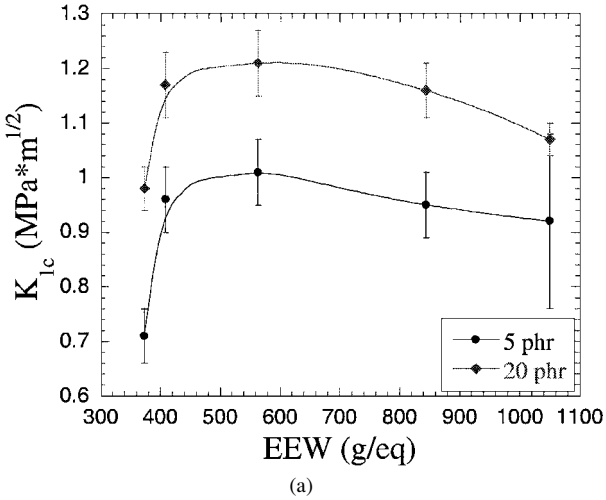

(a)

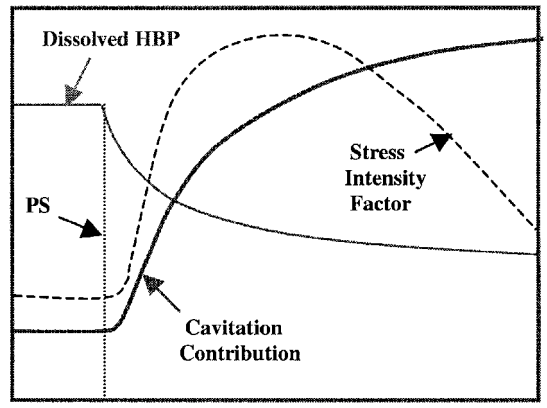

(b)

Figure 9 (a) Fracture toughness (K_{1c}), plotted versus HBP EEW for two different concentrations: 5 and 20 phr. (b) Combination of toughening mechanisms invoked to explain the maximum of K_{1c} at intermediate HBP functionality (EEW).

Fig. 9a shows the curve of K_{1c} versus the EEW of the different HBPs used for concentrations of 5 and 20 phr. As can be noted, at a content 20 phr, the BE2 (EEW = 373 g/eq.), which was totally compatible with the epoxy, already toughened the resin by 60% with respect to the neat resin ($K_{1c} = 0.6$). In this case, the increase in toughness was induced by a more flexible network containing segments with molecular weight double that of the neat resin (EEW = 187 g/eq.), and it is known that segmental mobility of cross-links in a thermoset strongly increases its toughness [26]. As soon as phase separation started, when a less functional HBP of an EEW of 408 g/eq was used, the K_{1c} increased. Further decrease in HBP functionality, led to a further increase in K_{1c}, which, then passed through a maximum and finally decreased to lower values. In order to understand why such a maximum in toughness was observed at middle HBP functionality, co-operation among the different toughening mechanisms should be considered, as shown in Fig. 9b. For very low EEW, i.e. high functionality, all the HBP blended with the epoxy remained dissolved with the epoxy within a continuous phase together. In this way, as previously discussed, the capability of the matrix to undergo plastic deformation

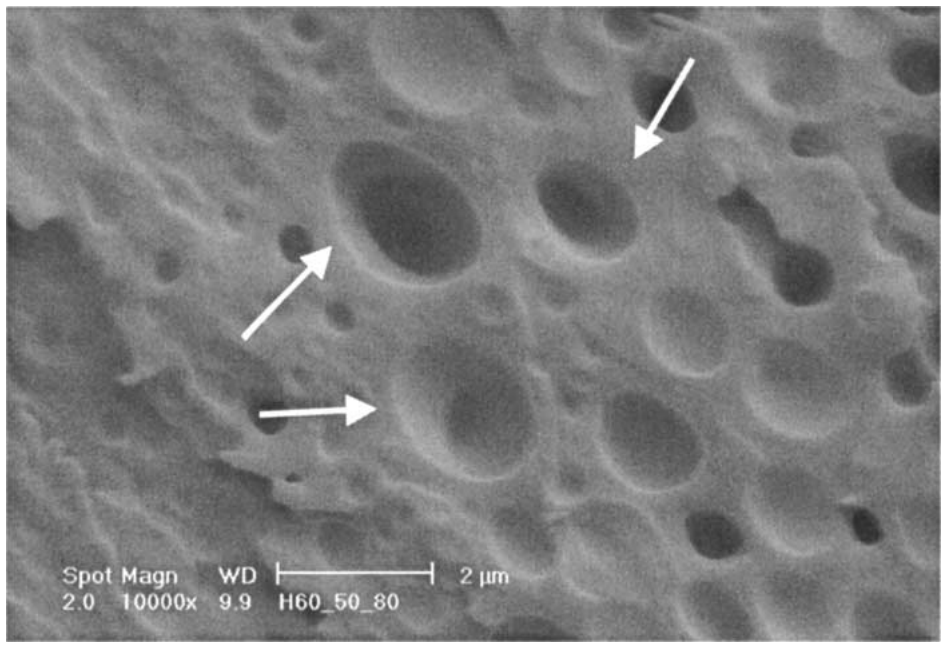

Figure 8 Partial cavitation occurring within a particle in a blend of 50 phr of HBP60 and DGEBA-IPD.

was increased, thus contributing to the final toughness through the only shear yielding mechanism. With the onset of phase separation, however, three main events were initiated.

First, particles were formed, which enhanced toughness by consuming energy when a void is created during the cavitation process. The more the EEW was increased the more efficient this mechanism became, since particles increased in volume and got stiffer, as shown previously in Table II.

At the same time however, the amount of residual HBP dissolved into the matrix started to decrease being ejected from the matrix into particles, and this effect became more pronounced the larger the EEW. As a consequence, the capability of the continuous phase to plastically deform was lowered with increasing incompatibility.

Finally, also the stress concentration versus EEW, which is caused by the presence of particles and relates to the extent of the area which can deform plastically with external load lower than the intrinsic matrix yielding stress, went through a maximum. In fact an initial increase in EEW corresponded to an increased number of particles and therefore a lower inter-particle-distance and a higher superposition of stress fields. However, with increasing stiffness of the particles, which was the case for high EEW (see Table II), the difference in moduli between matrix and particles decreased and as a consequence, the stress concentration was lowered, as expressed by Goodier equation [27].

In conclusion, all the different contributions to toughness summed together explain well why an optimum in toughness was observed using middle functionality of the HBPs, when the volume which phase separated was around 20% and the particles were stiff and still in the sub-micron size (0.5 μm).

3.5. Comparison with other modifiers

For the epoxy system investigated, the increase in K_{1c} for the optimum design of a HBP shell was found to be as high as 100%, as shown in Fig. 9a. The decrease in other thermo-mechanical properties was of 15°C for the T_g (where the neat resin T_g is 170°C) and 10% for the Young's modulus, respectively. These results are in agreement with previous results obtained by Boogh *et al*. for different epoxy systems [8] and confirm that the use of HBPs as tougheners in epoxy resins is particularly efficient. However, since the achievement of good toughness performances with any kind of modifier is system sensitive, the results obtained with HBPs were compared in this work with the toughness enhancement obtained by a traditional CTBN modifier frequently used to increase fracture toughness in epoxies: the Hycar 1300 × 8 [28].

Table III compares the results obtained with 20 phr of Hycar 1300 × 8, and 20 phr of HBP60 in DGEBA-IPD cured at 100°C and post-cured at 180°C. It is worth noting that, hyperbranched polymers were more efficient than rubber in toughening, since a K_{1c} of 1.21 was obtained compared to 1.07 for the CTBN modifier, corresponding to a fracture toughness value of 530 and 400 J/m^2 respectively. At the same time, both modifiers lowered the other thermo-mechanical properties such as Young's modulus and glass transition temperature, by the same amount. Finally Table III highlights the advantages of hyperbranched polymers for polymer processing: for the Hycar modifier had a viscosity ten times greater than that of HBP60, which, for a typical concentration of 20 phr, results in obvious disadvantages in terms of processing.

4. Conclusions

Varying the shell surface chemistry is a very powerful tool for designing final properties, and is new and unique to hyperbranched polymer molecules. The thermo-mechanical properties of the continuous and dispersed phase, toughening mechanisms and toughness optimisation in hyperbranched polymer epoxy blends were thus investigated as a function of HBP shell chemistry. Optimum mechanical properties were obtained for medium functionalities of the HBP, to which finely dispersed particles correspond, in a suitable size range for toughening. At the same time, a pronounced residual miscibility of the modifier within the matrix enhanced energy consumption by plastic deformation. Particle properties were evaluated by first calculating the composition through Fox equation and then glass transition temperature and stiffness. Results showed that the second domain particles can be either rubber-like or glass-like, depending on the shell chemistry of the HBP. Due to the high reactivity of these molecules, good adhesion between particles and matrix was ensured, allowing the particles to undergo extensive cavitation without any debonding. Coupling this effect with plastic deformation of the matrix, an increase in fracture toughness up to 100% was achieved with only 20 phr of HBP. Furthermore, this increase in fracture toughness corresponded to a decrease of only 10% in Young's modulus and of 15°C in glass transition temperature. Other modifiers, such as CTBN rubbers, showed less efficient performance in fracture toughness coupled with a lower processability, due to lower particle-matrix adhesion and lower particle rigidities on one hand, and a higher viscosity on the other.

Acknowledgements

Perstorp Specialty Chemicals is acknowledged for their financial support. Dr Christopher Plummer and Dr Louis Boogh are gratefully acknowledged for their contribution to fruitful discussions.

References

1. R. N. HAWARD and D. R. J. OWEN, *J. Mater. Sci.* **8** (1973) 1136.
2. J. N. SULTAN and F. J. McGARRY, *Polym. Eng. Sci.* **13** (1973) 29.
3. S. C. KUNZ, J. A. SAYRE and R. A. ASSINK, *Polymer* **23** (1982) 1897.
4. X. H. CHEN and Y. W. MAI, *J. Mater. Sci.* **34** (1999) 2139.
5. C. B. BUCKNALL and I. K. PARTIDGE, *Polymer* **24** (1982) 639.
6. D. VERCHERE, H. SAUTEREAU, J. P. PASCAULT, S. M. MOSCHIAR, C. C. RICCARDI and J. J. WILLIAMS, *J. App. Polym. Sci.* **41** (1990) 467.
7. A. J. KINLOCH and D. L. HUNSTON, *J. Mater. Sci. Lett.* **6** (1987) 137.

8. L. BOOGH, B. PETTERSSON and J. A. E. MÅNSON, *Polymer* **40** (1999) 2249.
9. R. MEZZENGA, L. BOOGH, B. PETTERSSON and J. A. E. MÅNSON, *Macromol. Symp.* **149** (2000) 17.
10. R. MEZZENGA, C. J. G. PLUMMER, L. BOOGH, B. PETTERSSON and J. A. E. MÅNSON, *Polymer* **42** (2001) 305.
11. R. MEZZENGA, L. BOOGH and J. A. E. MÅNSON, in Proceedings of Deformation Yield and Fracture of Polymers, Cambridge, April 2000, p. 55.
12. T. G. FOX, *Bull. Am. Phys. Soc.* **1** (1956) 123.
13. Z. HASHIN, *J. Appl. Mechanics* **29** (1962) 143.
14. Y. HUANG and A. J. KINLOCH, *J. Mater. Sci.* **27** (1992) 2753.
15. X. H. CHEN and Y. W. MAI, *ibid.* **33** (1998) 3529.
16. F. J. GUILD and A. J. KINLOCH, *ibid.* **30** (1995) 1689.
17. F. J. GUILD and R. J. YOUNG, *ibid.* **24** 2454 (1989).
18. D. S. DUGDALE, *J. Mech. Phys. Solids* **8** (1960) 100.
19. C. B. BUCKNALL, "Toughened Plastics" (Applied Science Publishers, London, 1977).
20. Y. HUANG and A. J. KINLOCH, *J. Mater. Sci.* **27** (1992) 2763.
21. T. FUKUI, Y. KIKUCHI and T. INOUE, *Polymer* **32** (1991) 2367.
22. W. D. BASCOM, R. Y. TING, R. J. MOULTON, C. K. RIEW and A. R. SIEBERT, *J. Mater. Sci.* **16** (1981) 2657.
23. A. LAZZERI and C. B. BUCKNALL, *ibid.* **28** (1993) 6799.
24. C. FOND, A. LOBBRECHT and R. SCHIRRER, submitted.
25. C. B. BUCKNALL, D. S. AYRE and D. J. DIJKSTRA, *Polymer* **41** (2000) 5937.
26. A. J. KINLOCH, C. A. FINCH and S. HASHEMI, *Polym. Comm.* **28** (1987) 323.
27. J. N. GOODIER, *J. Appl. Mech.* **55** (1933) 39.
28. A. F. YEE and R. A. PEARSON, *J. Mater. Sci.* **21** (1986) 2462.

Received 25 October 2000
and accepted 13 June 2001